



Femtosecond photoswitching dynamics and microsecond thermal conversion driven by laser heating in FeIII spin-crossover solids.

Roman Bertoni, Maciej Lorenc, A. Tissot, M.L. Boillot, Eric Collet

► To cite this version:

Roman Bertoni, Maciej Lorenc, A. Tissot, M.L. Boillot, Eric Collet. Femtosecond photoswitching dynamics and microsecond thermal conversion driven by laser heating in FeIII spin-crossover solids.. Coordination Chemistry Reviews, 2015, 282-283, pp.66-76. 10.1016/j.ccr.2014.05.024 . hal-01005418

HAL Id: hal-01005418

<https://univ-rennes.hal.science/hal-01005418>

Submitted on 12 Jun 2014

HAL is a multi-disciplinary open access archive for the deposit and dissemination of scientific research documents, whether they are published or not. The documents may come from teaching and research institutions in France or abroad, or from public or private research centers.

L'archive ouverte pluridisciplinaire **HAL**, est destinée au dépôt et à la diffusion de documents scientifiques de niveau recherche, publiés ou non, émanant des établissements d'enseignement et de recherche français ou étrangers, des laboratoires publics ou privés.

Edited May 24

Femtosecond photoswitching dynamics and microsecond thermal conversion driven by laser heating in Fe^{III} spin-crossover solids.

R. Bertoni,^a M. Lorenc,^a A. Tissot,^b M.-L. Boillot,^b E. Collet^{a,*}

^aInstitut de Physique de Rennes, UMR UR1-CNRS 6251, Université Rennes 1, 35042 Rennes, France

^bInstitut de Chimie Moléculaire et des Matériaux d'Orsay, UMR-CNRS 8182, Université Paris-Sud, Orsay, France.

*Corresponding author: Tel.: +33 223236532 Fax: +33 2 23236717.

E-mail address : eric.collet@univ-rennes1.fr (E. Collet)

Contents

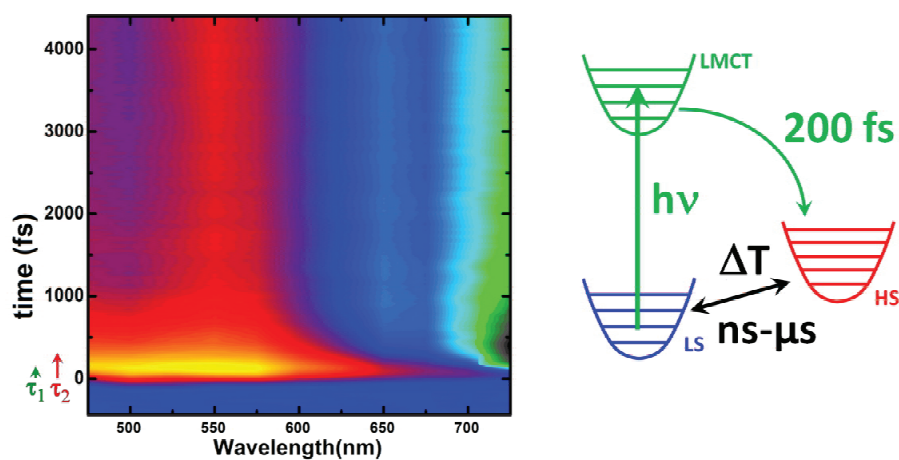
1	Introduction
2	The different thermal spin crossover of the investigated Fe(III) compounds
3	Ultrafast photoswitching
3.1	Results
3.2	Discussion
4	Spin-state switching driven by lattice expansion and heating
4.1	Results
4.2	Discussion
4.3	Comparison between strongly and weakly cooperative crystals
5	Conclusion
6	Experimental section
	Acknowledgements
	References

Abstract

In this paper we review time-resolved studies of ultrafast light-induced spin-state switching, triggered by a femtosecond laser flash, and the following out-of-equilibrium dynamics in Fe^{III} spin-crossover crystals. The out-of-equilibrium dynamics involves several steps, resulting from the ultrafast molecular photoswitching of low-spin (LS) to high-spin (HS) states in solids. First, the transient HS state is reached within 200 femtoseconds, and may rapidly decay into the stable LS state of the system. A second process at longer delay, associated with volume expansion, drives additional conversion to the HS state during the so-called elastic step occurring at nanosecond time scale. Finally, the laser heating process induces a temperature jump in the crystal that may result in a significant thermal population of the HS state on microsecond time scale. The photoswitching mechanism is of local nature and has linear dependence on the excitation fluence, whereas the heating effect can macroscopically perturb the LS/HS equilibrium. We discuss similarities and differences between photoswitching dynamics in solution and in different crystals for which the thermal spin conversion is of more or less pronounced cooperative nature.

Edited May 24

Graphical abstract



Highlights

Ultrafast spectroscopy reveals spin-state photo-switching in molecular crystals

Keywords: Spin-crossover; Intersystem crossing; Radiationless relaxation; femtosecond spectroscopy; ultrafast spectroscopy

Edited May 24

1. Introduction

Bridging the gap between molecular photoswitching in solution [1,2,3] and photoinduced phase transition in the solid state [4,5] is important for the development of photo-active materials. Indeed, bistable molecules in solution exhibit a wealth of light-induced transformations, which may give rise to inter- or intra-molecular chemical reactions [6], electron transfer [7,8] or changes of the molecular states [9,10,11]. In molecule-based solids, light-induced phenomena are important for driving a material between different states associated with different macroscopic physical properties [12,13,14,15,16,17]. Femtosecond laser pulses are widely regarded as the most likely source for switching molecular solids on ultrafast timescale [18,19,20,21,22,23,24,25]. Among the latter, spin-crossover compounds (SCO) are prototypes of systems showing molecular bistability in the solid state, which may be converted from low-spin (LS) to high-spin (HS) states under various external perturbations. In these materials, the photoswitching under weak continuous light irradiation at low temperature was extensively studied [26,27], and few reports discussed the relaxation mechanism after nanosecond laser excitation [28,29]. Regarding the photoswitching dynamics of the SCO molecule itself, there exists a robust literature dealing with investigations on isolated SCO molecules in solution, using ultrafast optical, X-ray or Raman spectroscopies. Major developments by the groups of Chergui, McCusker, McGarvey, Hendrickson, Mathies, Schoenlein and others gave a comprehensive description of the subtle coupling between the changes of electronic states and the structural reorganization [30,31,32,33,34,35,36,37,38,39,40,41,42,43,44,45,46,47,48]. In the solid state, the interaction between molecules can give rise to more complicated phenomena, such as the appearance of striped structures of bi-stable spin-crossover molecules in HS and LS states, of periodic [49] or aperiodic nature [50]. The strong intermolecular coupling can also give rise to cooperativity and first-order phase transition [51] from purely LS to purely HS states with thermal hysteresis. Recently, nanosecond laser excitation demonstrated the possibility to generate LS to HS transition inside thermal hysteresis loop [29,52].

Ultrafast investigations of photo-transformations in crystals were later carried out for Light Induced Excited-Spin State Trapping (LIESST) [53] and more recently for reverse LIESST [54], and it was revealed that the crystal response to femtosecond excitation is a multi-step process [21]. By using ultrafast optical spectroscopy and time-resolved photocrystallography, we provided a comprehensive account of the sequence of events schematically represented in Fig. 1. The typical time-resolved optical data shown in Fig. 1 indicate a three-step dynamic [55,56,57,58,59,60], as the relative change of transmitted light intensity $\Delta I/I$ increases with the HS fraction. First, the absorption

Edited May 24

of light at the molecular level locally switches a small fraction $\Delta X_{HS}^{h\nu} \approx 1\%$ of molecules on the sub-picosecond timescale from LS to HS state. The fraction of HS molecules remains unchanged over to 1–10 ns as during this interval, but every photo-excited molecule releases heat through electron-phonon coupling and then phonon-phonon relaxation processes. This local process leads to lattice expansion shown in Fig.1b, observed by time-resolved x-ray diffraction [21,55,57,58], which occurs ≈ 50 ns after photo-excitation. During this elastic step, the second step in sequence, the fraction of HS molecules increases, as a result of the internal pressure due to lattice expansion[56,60]. However, this expansion is not instantaneous but rather limited by the propagation of elastic strain in the crystal (typically at the speed of sound). Finally, the last step resulting from the heating of the lattice by the laser flash is the thermal population of the HS state which occurs on the μ s regime. This heating is associated with an important increase of the Debye-Waller factor observed by x-ray diffraction (Fig. 1c).

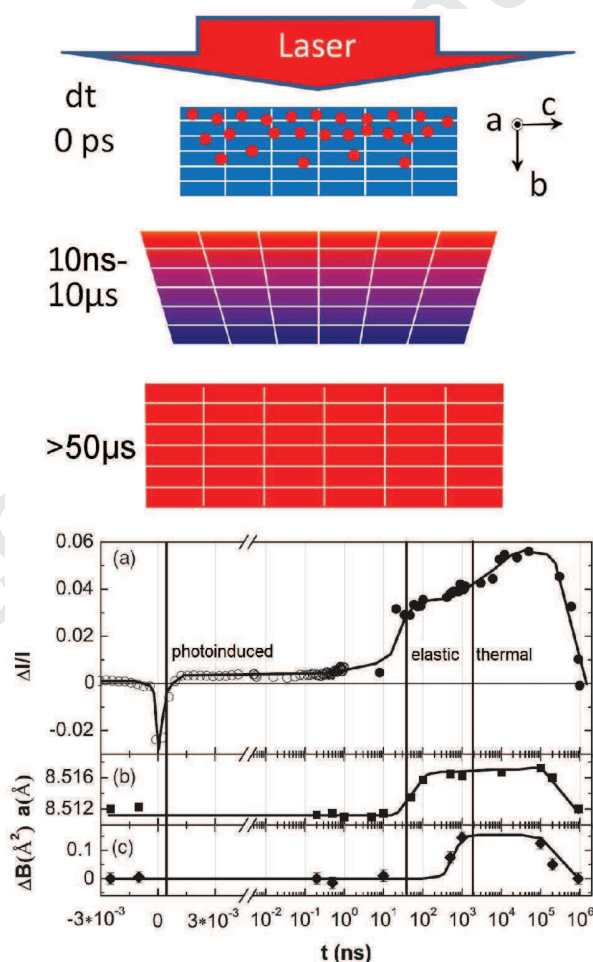


Fig. 1. Top: Schematic drawing of the dynamics. The laser deposits energy on photo-excited molecules (red dots) of the crystal at $dt = 0$ ps. The gradient of deposited energy results in an inhomogeneous lattice expansion in the 10 ns–10 μ s time window. At 50 μ s, the temperature is homogenized over the crystal and the

Edited May 24

heating effect results in thermal population of the HS state. (a) Differential intensity of transmitted probe light ($\Delta I/I$) measured at 600 nm on a single crystal of $[(\text{TPA})\text{Fe}(\text{TCC})]\text{PF}_6$ after femtosecond excitation at 800 nm at 200 K. (b), (c) Time-resolved x-ray diffraction experimental data: lattice parameter a (b) and variation of Debye-Waller factor B between $dt < 0$ and $dt > 0$ (c). Solid lines are drawn to guide the eyes. These figures were reproduced from ref. [55,58], with permission of the copyright holders.

Those studies dealt with non-cooperative materials undergoing thermal conversion of crossover type [61]. One may wonder if the abovementioned multi-step dynamics is still valid for cooperative materials undergoing first-order phase transition, and how the response differs in the time domain with regard to non-cooperative systems. Here we present a review of the results obtained in four Fe(III) spin-crossover complexes (Fig. 2). The two first samples are $[\text{Fe}(\text{3-MeO-SalEen})_2]\text{PF}_6$ single crystals (**1**), nano-crystals (**2**), H-3-MeO-SalEen being the condensation product of 3-methoxy-substituted salicylaldehyde and N-ethyl-ethylenediamine. The two others are catecholato-Fe(III) $[(\text{TPA})\text{Fe}(\text{TCC})]\text{PF}_6$ single-crystals, where TPA = tris(2-pyridylmethyl)-amine and H_2TCC = 3,4,5,6-tetrachlorocatecholate, of the monoclinic (**3**) and orthorhombic modifications (**4**) [61]. As shown in Fig. 2, (**1**) undergoes a first-order spin transition with small hysteresis, whereas (**2**), (**3**) and (**4**) undergo more gradual conversions. We also present complementary results to those already reported for (**1**).

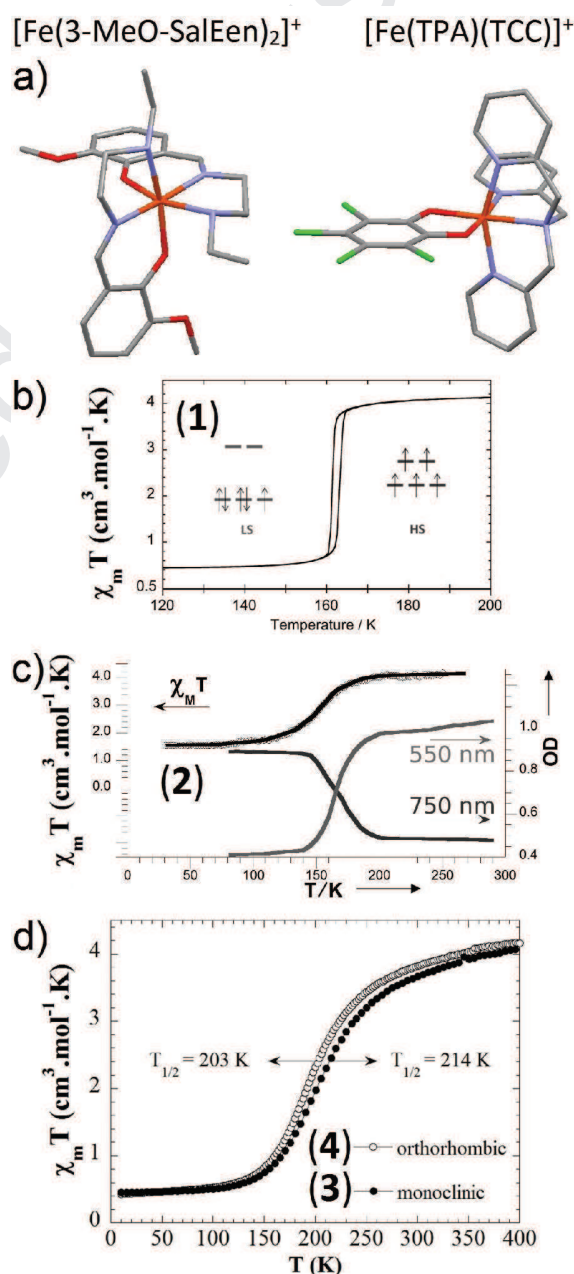


Fig. 2. The $[\text{Fe}(\text{3-MeO-SalEen})_2]^+$ and $[(\text{TPA})\text{Fe}(\text{TCC})]^+$ cations. $\chi_M T$ versus T plots are given for single crystals (**1**, a) and nanocrystals (**2**, c) of $[\text{Fe}(\text{3-MeO-SalEen})_2]\text{PF}_6$ and for the monoclinic (**3**, d) and orthorhombic (**4**, d) forms of $[(\text{TPA})\text{Fe}(\text{TCC})]\text{PF}_6$. Figures were reproduced

Edited May 24

from ref. [53,61,62], with permission of the copyright holders.

Accepted Manuscript

Edited May 24

2 The different thermal spin conversion of the investigated Fe(III) compounds

Single crystals of **(1)** are shown in Fig. 3a. This complex was initially synthesized by Hendrickson group [63], and its crystalline form undergoes a first-order transition between LS ($S=1/2$) and HS ($S=5/2$) states around 162 K [62]. It is characterized by a discontinuous evolution of the $\chi_M T$ vs. T curve (χ_M = molar magnetic susceptibility, T = temperature) in relation with the spin-state switching (Fig. 2b). This discontinuous conversion, associated with a narrow thermal hysteresis, is the signature of a strongly cooperative process. A detailed study of the phase transition at thermal equilibrium and of the associated structural changes involved is presented in ref [62].

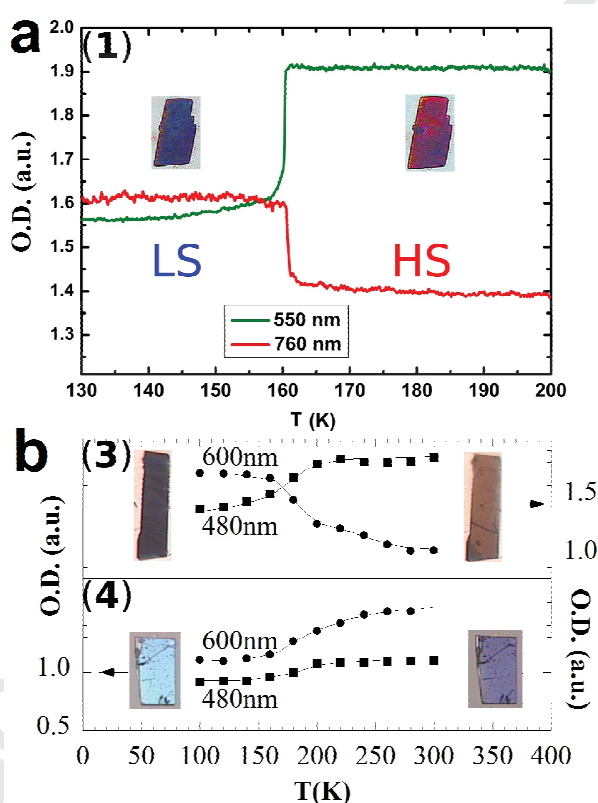


Fig. 3. Temperature dependence of the optical density at 550 and 760 nm for a 20 μm thin single crystal of **(1)**, **a**) and at 480 and 600 nm for single crystals of **(3)**, **b**) and **(4)**, **b**). Photographs were made in pure LS and HS states. Figure 3a b was reproduced from ref. [61], with permission of the copyright holders.

Edited May 24

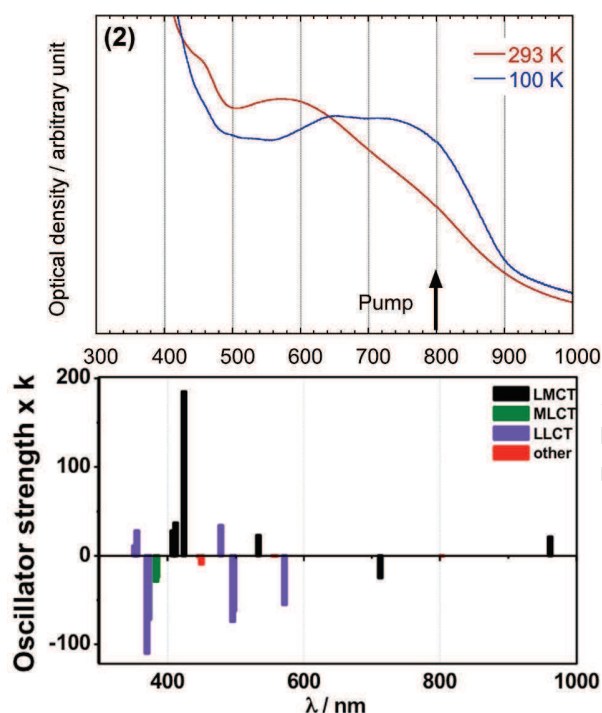


Fig. 4. Optical spectra of (1) recorded as a function of temperature. The TD-DFT calculations [64] reported for $[\text{Fe}^{\text{III}}(\text{pap})_2]^+$ (H-pap, tridentate $[\text{N}_2\text{O}]$ Schiff-base), a close analogue of (1, 2) provide the typical energies and oscillator strengths (for shake of clarity, $k = (-1)^n \times 10^3$) of LS ($n=1$) and HS ($n=0$) electronic absorptions of a Fe^{III} Schiff-base complex. The labels correspond with charge transfer (CT) electronic transitions involving ligand (L), metal (M) centered frontier orbitals (for instance ligand-to-metal charge transfer, LMCT) while the 'other' label means dd transitions.

The single-crystal material (1) shows thermochromism from dark blue to orange, characterized by the discontinuous change of optical density (OD), shown in Fig. 3a at 550 and 760 nm, associated with the discontinuous thermal transition from pure LS to pure HS state around 162 K. Optical measurements performed on nanocrystals of this compound (2) processed in transparent polymeric films revealed the associated spectral changes (Fig. 4). It corresponds with an increase of OD on HS LMCT (ligand to metal charge transfer) band centered around 550 nm and a decrease on another LMCT band centered around 750 nm [53], an assignment confirmed by the theoretical works by Cano and Ando on the same class of compound. The related data (energy and oscillator strength) in Fig. 4 also show the distinct Charge-Transfer (CT) components between Ligand (L) and Metal (M): LMCT at low energy, LLCT and MLCT at higher energy, resulting in the NIR-VIS absorption features (at c.a. 800, 550 and 400 nm) [64,65]. Sample (2), a nano-crystals assembly of the $\text{Fe}(\text{III})$ complex $[\text{Fe}(\text{3-MeO-SalEen})_2]\text{PF}_6$ in a polymeric matrix, undergoes a thermal spin-crossover between LS and HS states centered at $T_{1/2} = 156$ K, as indicated by the change in magnetic susceptibility and color (Fig. 2c, Fig. 3a). It shows a loss of first-order character in comparison with macroscopic single crystals. As the

Edited May 24

nanocrystals are embedded in a PVP film, this effect is attributed to particle-matrix interactions [66]. The temperature dependence of the $\chi_{\text{M}}T$ product for **(3)** and **(4)** are typical for gradual thermal crossover from low temperature $S=1/2$ (LS) to high temperature $S=5/2$ (HS) states (Fig. 2d). The characteristic temperatures corresponding to 50% conversion are $T_{1/2} \approx 214$ K for **(3)** and ≈ 203 K for **(4)**. This shift results from the different molecular packing between the polymorphs **(3)** and **(4)**. Their optical properties also differ during the LS to HS conversion: **(3)** changes from dark violet to orange whereas **(4)** changes from light blue to dark blue (Fig. 3b) and the optical density at 600 nm decreases for **(3)** and increases for **(4)**.

These changes of OD, commonly used for monitoring the thermal evolution of the HS population, are used here for tracking the evolution of the fraction of molecules in the HS state in time by using the transient absorption pump-probe method described in ref [55] (experimental section hereafter).

3 Ultrafast photoswitching

We performed ultrafast studies of photo-switching of these materials by exciting with fs laser pulse these compounds on the LMCT band related to the LS state, that is located on the low energy side of absorption bands as established (i) from the relative LS and HS absorption intensities, (ii) by comparison with oscillator strength calculations in an analogue of **(2)** (Fig 4). The typical time-resolved data shown in Fig. 1 and obtained for **(3)**, evidence the sub-picosecond timescale from LS to HS state photoswitching. In the section below, we analyze in detail the sub-picosecond photo-switching process for the different Fe(III) compounds.

3.1 Results

We compare in Fig. 5 new results of the photoswitching dynamics for **(1)**, for which previous fs studies indicated changes of optical transmission on 200 fs time scale [62], with the results already reported for **(2)**, **(3)** and **(4)**. For **(1)**, the evolution of OD, ΔOD , following fs laser excitation of **(1)** indicates two main steps. A transient peak appears immediately after excitation and ΔOD settles onto a plateau in the second step on a timescale shorter than 1 ps. As for the spectroscopic study performed on **(2)** (Fig 5b, [53]) ΔOD increases at 550 nm and decreases at 760 nm for single crystals (Fig 5a), which is a direct signature of HS state formation, in good agreement with changes of OD observed at thermal equilibrium from the LS to HS states (Fig. 3a). For **(3)** and **(4)** similar 2-step processes are observed with a dynamical process complete at the ps timescale (Fig. 5c). In these low symmetry crystals, the OD strongly depends on the direction of light polarization with respect to crystalline axis, as discussed in details for **(3)** and **(4)** [61]. This is also the case for **(1)** but we were not

Edited May 24

able to perform a polarization analysis because of the too high extinction coefficient of single crystals. Therefore, we only measured with the polarization allowing maximal transmitted signal.

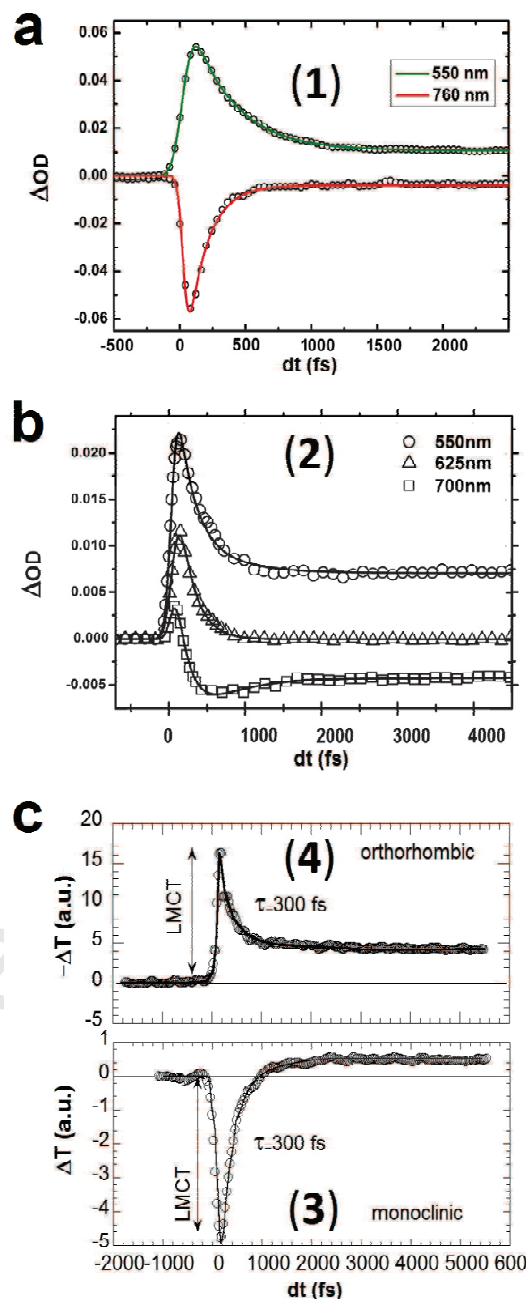


Fig.5. Kinetic traces of ΔOD obtained by two-color pump-probe experiment for (1, a) and (2, b) and of the increase of transmission ΔT for (3, c) and decrease of transmission $-\Delta T$ for (4, c). Fits with the mono-exponential model (solid lines) give $\tau = 330 \pm 40$ fs at 550 nm and $\tau = 180 \pm 40$ fs at 760 nm for (1), $\tau = 350 \pm 40$ fs at 550 nm and $\tau = 200 \pm 40$ fs at 625 nm for (2), $\tau = 300 \pm 40$ fs at 600 nm for (3) and (4). Figures were reproduced from ref. [53,58], with permission of the copyright holders.

Edited May 24

3.2 Discussion

The two dimensional time–wavelength plot of ΔOD following femtosecond laser excitation is shown in Fig. 6 for (2) [53]. It provides the spectroscopic signatures of the states involved in the two sub-ps steps. The transient absorption band which appears immediately after laser excitation, is characteristic of the excited electronic states. The plateau reached with a time constant shorter than one picosecond is associated with spectral features corresponding to positive ΔOD in VIS and negative ΔOD in NIR, revealing the formation of HS state in agreement with Fig. 4. The transient response recorded during the first 100 fs differs significantly, with a broad and strong absorption band dominating the VIS–NIR spectrum, indicating that the observed transient species are neither LS nor HS. It was deduced from these observations (Fig. 6) that the HS formation mechanism involves a short-lived excited state resulting from the population of the LMCT and other possible intermediate excited states (denoted INT, see below).

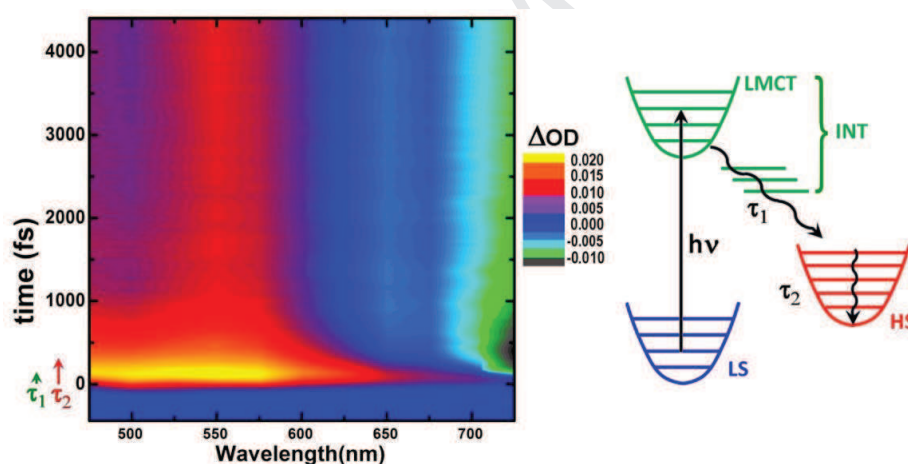


Fig. 6. 2D time–wavelength plot of ΔOD after femtosecond laser excitation for (2) and schematic representation of the photoswitching pathway with time constants τ_1 for the relaxation of short-lived intermediate states (INT), and τ_2 for the vibrational cooling of the photoinduced state. Figure was reproduced from ref. [53], with permission of the copyright holders.

In Fe(III) compounds the low-energy excitations of LS state, promote charge-transfer between the electronic configuration $L^2 t_{2g}^5 e_g^0$ like (or more precisely $L^2 d_{\pi}^5 d_{\sigma}^0$), where L refers to symmetry-adapted and occupied molecular orbitals centered on ligands, and an electronic configuration $L^1 t_{2g}^6 e_g^0$ like (or $L^1 d_{\pi}^6 d_{\sigma}^0$). Therefore, the femtosecond pump pulse leads to a LMCT Franck-Condon excited state that relaxes through intersystem crossing, and possibly via different intermediate states, to the

Edited May 24

HS state (Scheme Fig 6). For single crystal, we could not perform broadband spectroscopy because of the high absorption in the VIS range, but data in Fig. 5a evidence the transient peak resulting from the instantaneous population of LMCT state. The simple model used here for reproducing the kinetics of this photoswitching from LS to HS states in single crystals only considers a global intermediate state corresponding to the fast decay from the LMCT state to the final HS state. Therefore we describe the population of the HS state with a time constant τ . For the fitting procedure, we convoluted this exponential decay with the Gaussian IRF of our experiment (140 fs) and we found $\tau = 180 \pm 40$ fs for the ΔOD time trace at 760 nm in quite good agreement with $\tau = 200 \pm 20$ fs reported for (2)[53]. For the ΔOD time trace at 550 nm we found a longer time constant $\tau = 330 \pm 40$ fs. This is due to the fact that the single exponential model used here is too simple for reproducing the kinetics of this photoswitching process. Indeed, it was shown in nanocrystals that the dynamics is better described over a broad spectral range with a bi-exponential model, for which a fixed time constant τ_1 (of 200 fs) describes the population of the HS state by the depopulation of intermediate (INT) electronic states and a longer time constant τ_2 describes the vibrational cooling of the hot HS state, associated with a global spectral narrowing (Fig. 6). By analyzing the data in this way, both measurements on single crystals and nanocrystals indicated that the time traces of OD at 550 nm also include some vibrational cooling signature with a time constant τ_2 of 500 fs, giving an overall apparent τ for reaching the final HS state of 350 fs (Fig. 5 and 6).

The femtosecond optical studies reported for (3) and (4) shown in Fig. 5c lead to similar conclusion: a transient absorption peak appears for both polymorphs due to a LMCT state. We show the time dependent optical transmission at 600 nm between negative and positive delays, varying in opposite directions for the two polymorphs (ΔT is shown for (3) and $-\Delta T$ for (4)) between LS and HS states, confirm the formation of HS states. Here again we observe for both compounds, an exponential-like population of the HS state, which proceeds from the LMCT state with a 300 fs time constant.

The initial step of LS–HS conversion in solids is therefore equally fast as the one observed for other spin-crossover molecules in solution. This is due to the local nature of structural trapping of the electronic excited state. But a very important aspect of SCO solids resides in revealing cooperativity or non-linear response of such systems to light excitation, which indeed is the case for some molecular materials [5,20,67,68,69]. The response of a single crystal (1) to different excitation fluencies, during the ultrafast photoswitching step performed at 140 K is shown in Fig 7a. The fraction of molecules photo-switched to the HS state, $X_{HS}^{h\nu}$, was estimated from ΔOD on the plateau at picosecond timescale. It shows a clear linear dependence with the excitation fluency F . In addition, a fluency $F = 100 \mu J/mm^2$ in the probed volume corresponds typically to $3 (\pm 1)$ photons per 100

Edited May 24

molecules. As the fraction of these molecules converted from LS to HS state is 2.5 (0.5) %, it comes out that the efficiency of the process is very high (nearly every absorbed photon switches one molecule from LS to HS states). However, we could not detect any cooperative or self-amplification response during the course of ultrafast photoswitching dynamics, despite the fact that this crystal shows a strongly cooperative behavior at thermal equilibrium. This linear response to excitation density was already reported for the non-cooperative Fe^{III} SCO material (**3**) [58] (Fig. 7b) and was proportional to the fraction of molecules in the LS state prior to photo-excitation [55,60]. All these observations underline the fact that the photoswitching, which occurs within less than 1 ps, can be regarded as independent local molecular events both for spin-crossover and spin-transition single crystals as none of them show self-amplification on the ps timescale.

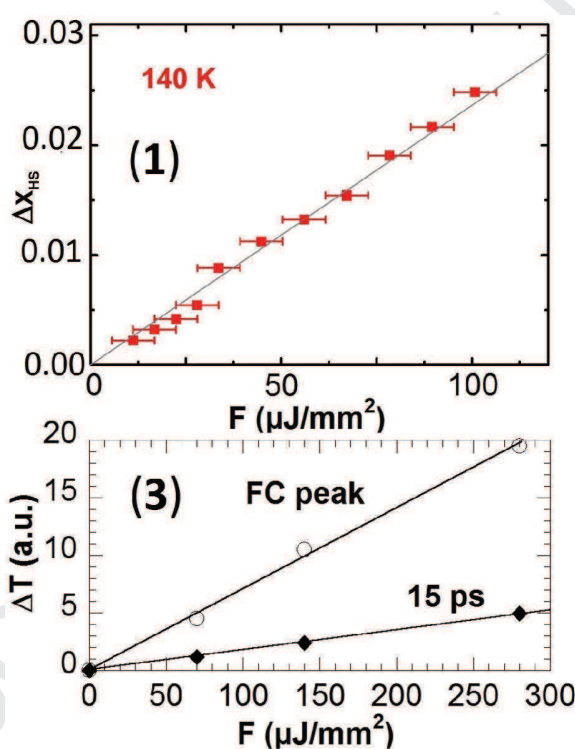


Fig.7. Fluency dependence of the fraction of molecules photo-converted to the HS state at 140 K for (**1**) after irradiation at 850 nm of a 20 μm thick single crystal, and of the photo-response on the LMCT Franck-Condon peak and transmission variation at 15 ps for (**3**). Part of the figure was reproduced from ref. [58], with permission of the copyright holders.

Edited May 24

4 Spin-state switching driven by lattice expansion and heating

After the photoswitching process discussed above, a complex out-of-equilibrium dynamics takes place, involving consecutive processes. Because of the local photo-switching, an internal pressure sets in, resulting from the molecular swelling (as Fe-ligand bonds expand). Time-resolved X-ray absorption spectroscopy of SCO molecules in solution and fs x-ray diffraction experiments in crystals also demonstrated that the Fe-ligand bonds elongate on the ≈ 200 fs timescale [70,71,72,73]. In addition, this photoswitching induces lattice heating as every photo-excited molecule releases energy through electron-phonon coupling and then phonon-phonon relaxation processes. Both effects drive lattice expansion, which was observed to occur after ≈ 50 ns by time-resolved x-ray diffraction in (4) [57,58] and in (3) [21,55,56] as shown in Fig. 8 c. This crystal expansion leaves space for other molecules to swell, promoting additional molecules into the HS state, as observed both by time-resolved x-ray diffraction (Fig. 8a) and optical spectroscopy (Fig. 1). However, this macroscopic expansion is not instantaneous but rather limited by the propagation of elastic strain in the crystal [57,58]. Finally, the heating of the lattice by the laser flash, associated with an important increase of the Debye-Waller factor observed by x-ray diffraction (Fig. 1c), is accompanied by the thermal population of the HS state, which occurs on the μ s regime.

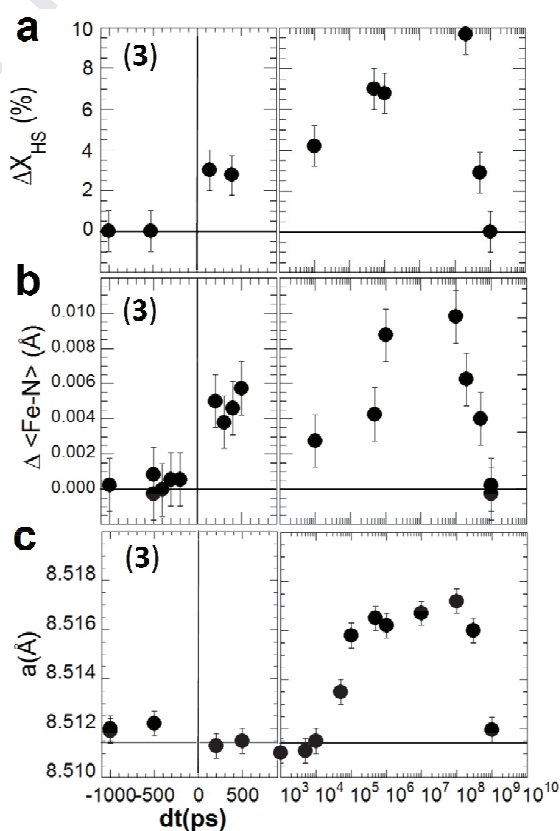


Fig. 8. Time dependence of the HS fraction (a), $\langle Fe-N \rangle$ bond length (b), and of the lattice parameter a (c) deduced from x-ray diffraction data for (3). Figures were reproduced from ref. [22,56], with permission of the copyright holders.

Edited May 24

4.1 Results

As discussed in the introduction, it is interesting to compare these slower elastic and thermal spin-state conversion in the different compounds and we adopted the strategy described in ref [55] (see experimental section hereafter). Fig 9 compares the photoresponse of the different single crystals (1), (3) and (4) of similar sizes on a time domain spanning from ps to ms. In these 3 systems, the following three-step process is clearly evidenced:

- the local spin state photoswitching, after the transient LMCT peak, corresponds with the first increase of the HS fraction of few percents (step "hv" in Fig 9), which occurs within less than 1 ps, as shown in Fig. 1.
- the elastic switching, which gives the second increase (step "el" in Fig.9) in the 10-100 ns time scale.
- the thermal population of the HS state (step "th" in Fig.9), with the third increase at μ s time scale.

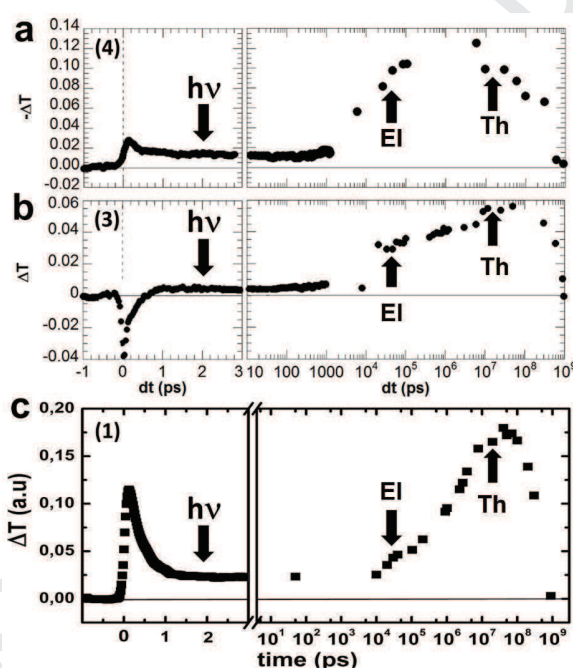


Fig. 9. Time dependence over several temporal scales of ΔT for (3, b) and $-\Delta T$ for (4, a) at 600 nm and (1, c) at 550 nm. The figures were partly reproduced from ref. [58], with permission of the copyright holders. "hv", "el" and "th" denote respectively the photo-induced, elastic and thermal steps.

Edited May 24

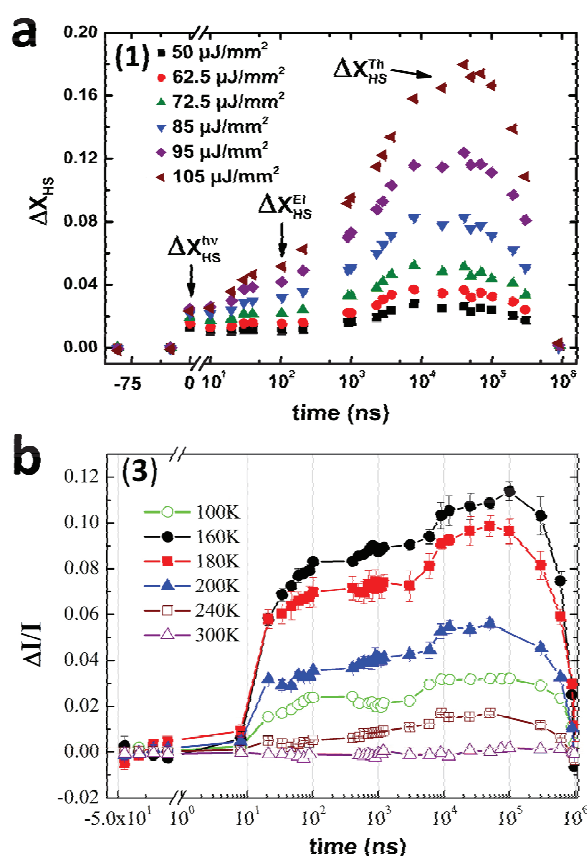


Fig.10.(a) Photo-excited fraction of HS molecules at 140K as a function of pump energy for (1) revealing the 3 steps of photoinduced (ΔX_{HS}^{hv}), elastic (ΔX_{HS}^{El}) and thermal (ΔX_{HS}^{Th}) nature and (b) photo-response of (3) for different temperatures. Figures were partly reproduced from ref. [55], with permission of the copyright holders.

Fig 10 shows how ΔX_{HS} evolves after fs laser excitation. The first time point measured at positive delay after laser excitation is 10 ps, when the local photoswitching dynamics towards the HS state presented in Fig. 4 is already complete. At this stage a fraction ΔX_{HS}^{hv} of molecules are converted from LS to HS and we note ΔX_{HS}^{El} and ΔX_{HS}^{Th} the HS conversion on the elastic and thermal steps respectively. On the one hand, we analyze in (1) the effect of excitation density and on the other hand the effect of temperature in (3).

For (3) the occurrence of significant thermal switching at the microsecond timescale is observed with a maximum response in the 160-180 K range. This results from two main effects described in detail in [55]: the temperature dependence of heat capacity, $C_p(T)$, and of $X_{LS}(T)$ the initial fraction of molecules in the LS state at a given temperature T . The optical energy absorbed by the crystal is redistributed over phonons during the relaxation process from the LMCT states to the lower lying HS state. This heat causes temperature increase ΔT on the macroscopic scale of the crystal, which occurs on μs time scale and is limited by heat diffusivity. After this global heating, the HS fraction reaches a transient equilibrium value $X_{HS}(T+\Delta T)$. But the amount of absorbed optical energy is proportional to

Edited May 24

$X_{LS}(T)$, the initial fraction of LS molecules, which is temperature dependent for (3) as it decreases in above 160 K with the gradual thermal conversion from LS to HS states. Therefore the temperature jump ΔT becomes smaller when X_{LS} decreases. This explains why the thermal conversion is more efficient at the beginning of the thermal crossover than at the crossover temperature.

For (1), upon the thermal step, the HS population is also higher than upon the photo-switching step. However, a complete conversion could not be reached by increasing the pump energy, due to sample damage. For this reason, the maximum conversion for (1) on the photo-switching step is $\Delta X_{HS}^{h\nu} \approx 2.5\%$ and the corresponding HS fraction thermally populated at $50\ \mu s$ is $\Delta X_{HS}^{Th} \approx 18\%$. The experimental values of $\Delta X_{HS}^{h\nu} = 0.007$ obtained for $[(TPA)Fe(TCC)]PF_6$ with $40\ \mu J/mm^2$ pulse, and $\Delta X_{HS}^{h\nu} = 0.025$ obtained for $[Fe(3-MeO-SalEen)_2]PF_6$ with $105\ \mu J/mm^2$ pulse are quite consistent and scale well with the excitation densities and the slight differences may come from the absolute OD (extinction coefficients, crystal thickness) and the uncertainties mentioned above.

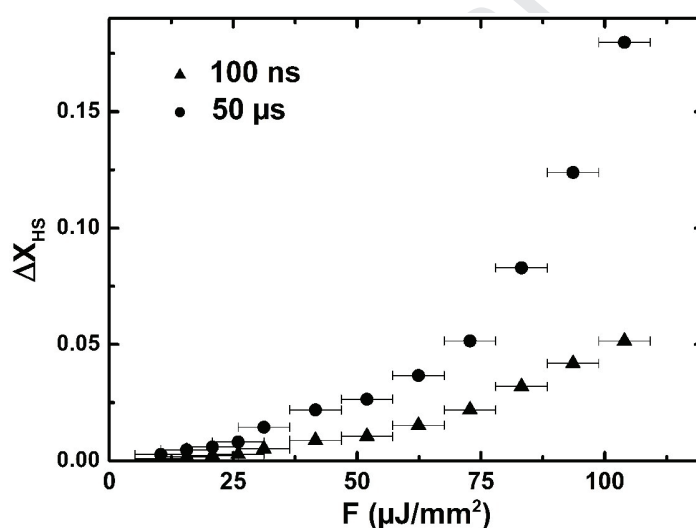


Fig.11. Evolution of the fraction of HS molecules on the elastic (100 ns) and thermal steps (50 μs) with the laser fluence, measured on (1) at $T = 140\ K$.

Fig. 11 shows how ΔX_{HS}^{El} and ΔX_{HS}^{Th} , the fraction of molecules populating the HS state on the elastic (100 ns) and thermal (50 μs) steps, change with respect to the excitation density for (1). This is a clear proof of the non-linear character of the elastic and thermal switching with the optical energy deposited on the crystal. The time dependence of the thermal HS population process ΔX_{HS}^{Th} for (1) showed in Fig. 12 follows an exponential like law. The different fits (continuous lines) performed for different excitation densities give an average value of $\approx 2.3(5)\ \mu s$ time constant. For the data shown in Fig. 12 with an initial temperature of 140 K, a temperature jump of 20 K for $105\ \mu J/mm^2$ fluency will correspond with a transient temperature of 160 K, whereas a $52.5\ \mu J/mm^2$ fluency will correspond

Edited May 24

with a temperature jump of 10K and transient temperature of 150K[55,58]. Given the accuracy of our data and the fact that the rate constants of the $LS \leftrightarrow HS$ equilibrium depend on temperature, this temperature change is not high enough to allow the detection of variations in the time constant.

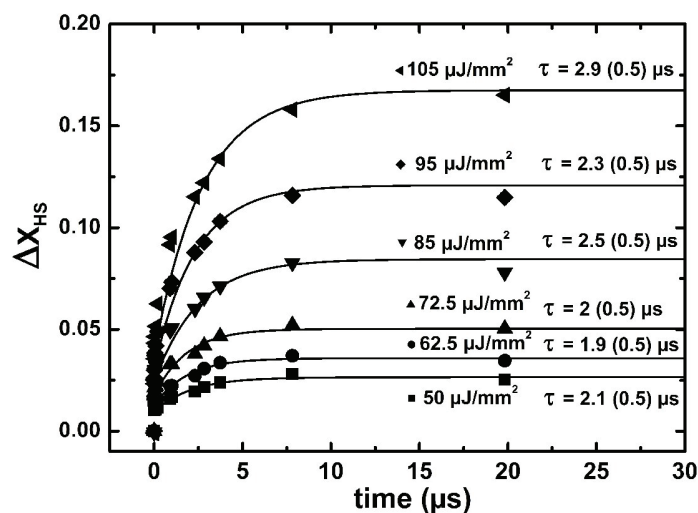


Fig.12. Thermal population of the transient HS state towards ΔX_{HS}^{Th} for (1).

4.2 Discussion

The data presented above mainly underline three effects in solids: the photoswitching process, the elastic step and the thermal population of the HS state. However, the HS state is not stable within the experimental condition set (140 K, ambient pressure) and we also observe the $HS \rightarrow LS$ relaxation. The kinetic of $HS \rightarrow LS$ relaxation and LS/HS out-of-equilibrium dynamics was already investigated in solution (around ambient temperature), using diverse methods including laser-flash photolysis,[74,75] Raman temperature jump techniques,[76] and ultrasonic relaxation[77]. These studies mainly focused on the $HS \rightarrow LS$ relaxation process, providing lifetime of the transient HS state of the order of 10-1000 ns (k_{HL} rate constants on the order of 10^6 - 10^8 s $^{-1}$). In the solid state, this relaxation can be very slow at low temperature and a broad distribution of SCO rate constants appears, which are sample and temperature dependent and can span from 10^{-14} to 10^9 s $^{-1}$ [27,37,64].

Fig. 13 shows the local $HS \rightarrow LS$ relaxation process of the photo-switched molecules in (1), observed on the ns time scale. For analyzing the relaxation dynamics we used an exponential fit, which yields ≈ 300 ps time constant ($k_{HL} \approx 3 \cdot 10^9$ s $^{-1}$). It can be compared to the results obtained by the laser flash photolysis technique developed by McGarvey and Lawthers to directly measure the rate at which spin-crossover complexes interconvert between the HS and LS states in solution[74]. This relaxation process is of intramolecular nature unlike the one shown in Fig. 14 related to the

Edited May 24

macroscopic 300 μ s relaxation dynamics of the crystal, which results from heating process following homogeneous/bulk excitation. The excess optical energy deposited on few molecules close to the surface of crystal (heterogeneous excitation) is converted to heat, which allows for a thermal population of the HS state, as the resulting temperature jump ΔT modifies the LS/HS equilibrium. Such population decays on the ns time scale. Nevertheless (as shown in the case of Fig. 14), the macroscopic and homogeneous temperature increase of the crystals is limited by heat diffusivity and thus occurs only on the μ s timescale[21,56] with the apparent 2.3 ± 0.5 μ s time constant for populating HS state.

Hauser explained that the LS to HS conversion may be regarded as tunneling for thermally populated levels LS vibrational states having large Franck Condon factors with the corresponding vibrational levels of HSstate [67]. There are two parameters that may explain the non-linear population of the HS state with respect to the optical energy absorbed by the crystal (Fig. 11). The first one is that the overlap between the vibrational levels of HS and LS states is higher when temperature is higher. The other one is that in cooperative systems the relative position in energy of the HS and LS potential depends on the HS fraction and therefore the increase of tunneling efficiency may be non-linear with the increase of the transient temperature. Finally, even though the laser penetration depth is in the range of crystal thickness, there may exist a gradient of deposited energy and it was also demonstrated that it takes μ s for the crystal to reach a homogeneous transient hot state[58]. This slow heat diffusivity may be the limiting factor for observing the thermal population of the HS state. As a transient temperature is reached in the crystal on the 50 μ s timescale, the new LS/HS equilibrium is reached, with a transient thermally populated HS fraction as high as $\Delta X_{HS}^{Th} \approx 18$ %. For such laser excitation densities, the temperature jump ΔT is in the 10-30 K range[55,57]. Therefore, the slower 300 μ s HS \rightarrow LS relaxation process observed in Fig. 14 is due to the recovery by the crystal of the initial temperature at equilibrium and this process is limited by the heat exchange between the sample and the cryostat as already underlined by Enachescu and Lorenc[21,28].

Edited May 24

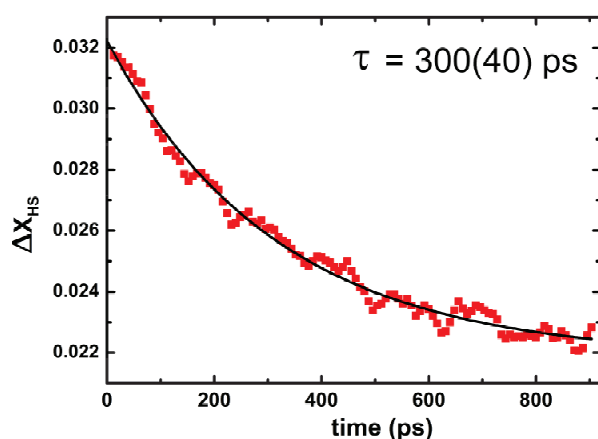


Fig.13. Molecular HS→LS relaxation switching dynamics in the ns range for $120 \mu\text{J}/\text{mm}^2$ excitation density at 140 K for (1)

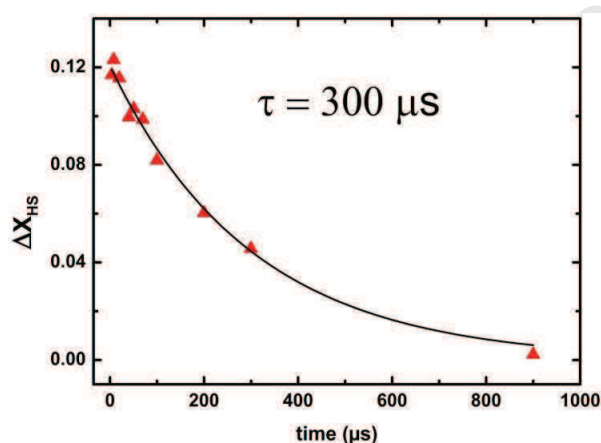


Fig.14. Macroscopic HS→LS relaxation due to sample thermalization at 140 K ($90 \mu\text{J}/\text{mm}^2$) for (1)

4.3 Comparison between strongly and weakly cooperative crystals

It is interesting to compare the out-of-equilibrium dynamics following photoswitching triggered by ultra-short light pulse obtained in a cooperative crystal showing a first-order phase transition to the ones reported in weakly cooperative crystals (Fig. 10).

Regarding the ultrafast LS-to-HS photoswitching step, the dynamics are similar: it occurs within ≈ 200 fs and the fraction of molecules photo-converted to the HS state changes linearly with the excitation density both for the present cooperative material (Fig. 7) and for weakly cooperative system. This local molecular transformation is similar to the one observed for molecules in solution.

Edited May 24

Regarding the elastic step, in weakly cooperative systems (Fig. 1), the internal pressure induced by the local process due to the "swelling" of molecules and lattice heating is ensued by volume expansion. During this elastic step the fraction of HS molecules strongly increases and becomes six times higher than the initial fraction of photo-switched molecules in the weakly cooperative solids **(3)** and **(4)** (Fig. 9). The amplitude of the elastic step in terms of HS conversion also depends on the difference between the crossover-and the working-point temperature, so the strong response in Fig. 1 is obtained in the vicinity of the crossover[55,60]. The elastic step results from the negative pressure (in the order of 300 bars [60]) due to the photoswitching process inducing both "swelling" of molecules and lattice heating. The mechanism is schematically represented in the left part of Fig. 15 with a (P,T) phase diagram. The experiment starts at a given temperature and ambient pressure marked by the white point, in the vicinity of the LS-HS crossover. On the timescale of the elastic step the HS state population is not thermally equilibrated as the propagation of heat requires μs delay. Therefore the temperature can be considered as constant for simplicity and thus the discontinuous white line represents the transformation path. The release of internal pressure ΔP , corresponding to a path towards negative pressure (Fig. 15) from a mainly LS (blue) state, favors an increase of HS (red) fraction by ΔX_{HS}^{El} . For the cooperative system presented here, the release of internal pressure ΔP is not high enough for reaching the HS phase. This may be possible with higher excitation density (associated with larger ΔP) or by performing the experiment at higher temperature, but exploring either of these cases is prohibited by irreversible damage (cracking) of the crystals.

Finally, on longer timescale (50 μs) the system settles to a transient equilibrium state with a transient higher temperature, corresponding to a new LS/HS equilibrium given by $X_{HS}(T+\Delta T)$. In the case of a cooperative material, this equilibrium is strongly modified in the vicinity of the phase diagram and the HS state is thermally populated with significant molecular fraction. In the case of **(1)** at 140K, a $\Delta T=22$ K temperature jump is sufficient to give rise to a complete conversion because of the abrupt LS-HS conversion at 162 K and this explains why the thermal response strongly increases with excitation density (Fig. 11). In the case of **(3)** and **(4)**, a 20 K temperature jump can only thermally populate a small fraction of HS state because of the more gradual thermal conversion (Fig. 2). At 140 K temperature jump larger than 100 K is required for reaching 80% conversion.

Edited May 24

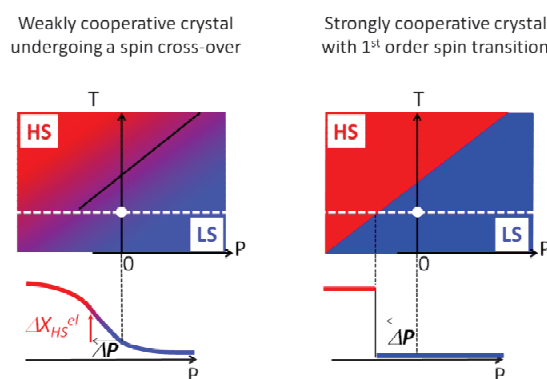


Fig. 15. The (P, T) phase diagram between LS (blue) and HS (red) regions, for weakly (left) and strongly (right) cooperative crystals. In the vicinity of the crossover (left) a negative pressure ΔP drives an increase of HS fraction by ΔX_{HS}^{el} . For a crystal with first order transition (right) this is not possible if ΔP is too small.

5 Conclusion

Molecular multistability in solution and in solids allows controlling molecular states by different stimuli and in particular by light excitation. The local molecular photoswitching in solids is very similar to that reported for molecules in solution, and even for the so-called cooperative solids we could not detect self-amplification process on the picosecond time scale. The concerted response of molecules in solids made it possible to identify two other mechanisms driving spin-state switching. One of elastic nature and one of thermal nature. The temperature jump resulting from laser excitation can give rise to a strong response in cooperative systems, which show discontinuous conversion at thermal equilibrium, but this response is more limited in systems showing more gradual response. These results underline the fact that the crystal is an active medium, which can give rise to self-amplification. While the process caused by temperature jump looks to some extent similar to the kinetics in solution, the role of elastic-driven transition is specific to the solid and needs to be further investigated.

6 Experimental section

The experimental details regarding already published material can be found in [62] for (1), [53] for (2), [21,55,56,58] for (3) and [57,58] for (4). The optical pump-probe experiments were configured in transmission geometry with quasi-collinear configuration. The complementary results presented here for (1) used the set-up described in [55], combining a mechanical translation stage to adjust the optical path difference for sub-ns measurements and the synchronization of two femtosecond

Edited May 24

amplifiers for 10ns-ms delays. In the new measurements on **(1)**, the pump wavelength was set to 850 nm on a LMCT band where it efficiently induces LS-to-HS transition (Fig 4). Single-wavelength transmission measurements at 550 and 760 nm probed the resulting LS-to-HS photoswitching dynamics by OD change, with an overall instrument response function (IRF) of ≈ 140 fs. In first order approximation, it is possible to extract ΔX_{HS} from ΔOD , if the absolute change of OD between HS and LS is known ($OD_{HS}-OD_{LS}$):

$$\Delta X_{HS}(t) = \frac{\Delta OD(t)}{OD_{HS}-OD_{LS}}$$

Experiments were performed on single crystals with typical dimensions of $(200 \pm 50) \times (300 \pm 50) \times (20 \pm 5) \mu\text{m}^3$. Both pump and probe light were parallel to the long crystal axis **a**, for which the penetration depth is maximal. The spot size of the pump beam had a diameter of 150 μm and the one of the probe was 80 μm to ensure the excitation homogeneity of the analyzed volume. The experiments were performed in the pure LS phase at 120 K and 140 K, far enough from the thermal transition temperature to avoid residual laser heating effects and high enough to ensure lifetime of the photoinduced HS state shorter than 1ms required for performing stroboscopic pump-probe measurements. Crystals were cooled down with a liquid nitrogen cryostream. Thenanocrystals samples **(2)** $(950 \pm 150) \times (270 \pm 40) \times (35 \pm 7) \text{ nm}^3$ were dispersed in a transparent PVP matrix. For **(3)**, the typical sample dimensions are $(400 \pm 50) \times (150 \pm 50) \times (20 \pm 5) \mu\text{m}^3$. For **(4)**, the typical sample dimensions are $(300 \pm 50) \times (200 \pm 50) \times (15 \pm 5) \mu\text{m}^3$.

Acknowledgements

This work was supported by the Institut Universitaire de France, Rennes Métropole, Région Bretagne (CREATE 4146), the ANR (ANR-13-BS04-0002) and Europe (FEDER).

References:

- [1] A. H. Zewail, *Angew. Chem. Int. Ed.* 112 (2000) 2688.
- [2] J.H. Lee, M. Wulff, S. Bratos, J. Petersen, L. Guérin, J.C. Leikman J.C., M. Cammarata, Q.Y. Kong, J. Kim, K. Moller, H. Ihee, *J. Am. Chem. Soc.* 135 (2013) 3255.
- [3] K. Haldrup, T. Harlang, M. Christensen, A. Dohn, T. Brandt van Driel, K. Skov Kjær, N. Harrit, J. Vibenholt, L. Guerin, M. Wulff, M. M. Nielsen, *Inorg. Chem.* 50 (2011) 9329.
- [4] K. Nasu, *Photoinduced phase transitions*, Ed. World Scientist, Singapore, 2004.
- [5] S. Koshihara & M. Kuwata-Gonokami Eds. *Special Topics in J. Phys. Soc. Jpn.* 75 (2006) 011001.
- [6] M. Kobayashi, S. Masaoka, K. Sakai, *Angew. Chem. Int. Ed.* 51 (2012) 7431.

Edited May 24

- [7] A. A. Bakulin, A. Rao, V. G. Pavelyev, P. H. M. van Loosdrecht, M. S. Pshenichnikov, D. Niedzialek, J. Cornil, D. Beljonne, R. H. Friend, *Science* 335 (2012) 1340.
- [8] C. D'amico, M. Lorenc, E. Collet, K.A. Green, K. Costuas, O. Mongin, M. Blanchard-Desce, F. Paul, *J. Phys. Chem. C* 116 (2012) 3719.
- [9] M. Iwamura, H. Watanabe, K. Ishii, S. Takeuchi, T. Tahara, *J. Am. Chem. Soc.* 133 (2011) 7728.
- [10] Y. Suffren, D. Zare, S.V. Eliseeva, L. Guénée, H. Nozary, T. Lathion, L. Aboshyan-Sorgho, S. Petoud, A. Hauser, C. Piguet, *J. Phys. Chem. C* 117 (2013) 26957.
- [11] F. Messina, M. Premont-Schwarz, O. Braem, D. Xiao, V. S. Batista, E.T.J. Nibbering, M. Chergui, *Angew. Chem. Int. Ed.* 52 (2013) 6871.
- [12] Y. Zhang, D. Li, R. Clérac, M. Kalisz, C. Mathonière, S. M. Holmes, *Angew. Chem. Int. Ed.* 49 (2010) 3752.
- [13] H. Jean-Ruel, R.R. Cooney, M. Gao, C. Lu, M.A. Kochman, C.A. Morrison, R. J. D. Miller, *J. Phys. Chem. A*, 115 (2011) 13158.
- [14] A. Bousseksou, G. Molnar, L. Salmon, W. Nicolazzi, *Chem. Soc. Rev.* 40 (2011) 3313.
- [15] H. Svendsen, J. Overgaard, M. Chevallier, E. Collet, B.B. Iversen, *Ang. Chem. Int. Ed.* 48 (2009) 2780.
- [16] S. Ohkoshi, K. Imoto, Y. Tsunobuchi, S. Takano, H. Tokoro, *Nature Chem.* 3 (2011) 564.
- [17] L. Catala, D. Brinzei, Y. Prado, A. Gloter, O. Stéphan, G. Rogez, T. Mallah, *Angew. Chem. Int. Ed.* 48 (2009) 183.
- [18] T. Ishikawa, N. Fukazawa, Y. Matsubara, R. Nakajima, K. Onda, Y. Okimoto, S. Koshihara, M. Lorenc, E. Collet, M. Tamura, R. Kato, *Phys. Rev. B*. 80 (2009) 115108.
- [19] B. Siwick, E. Collet, *Nature*, 496 (2013) 306.
- [20] M. Gao, C. Lu, H. Jean-Ruel, L. C. Liu, A. Marx, K. Onda, S. Koshihara, Y. Nakano, X. Shao, T. Hiramatsu, G. Saito, H. Yamochi, R. R. Cooney, G. Moriena, G. Sciaini, R.J.D. Miller, *Nature* 496 (2013) 343.
- [21] M. Lorenc, J. Hébert, N. Moisan, E. Trzop, M. Servol, M. Buron-Le Cointe, H. Cailleau, M. L. Boillot, E. Pontecorvo, M. Wulff, S. Koshihara, E. Collet, *Phys. Rev. Lett.* 103 (2009) 028301.
- [22] D. Boschetto, E. G. Gamaly, A. V. Rode, B. Luther-Davis, D. Glijer, T. Garl, O. Albert, A. Rousse, J. Etchepare, *Phys. Rev. Lett.* 100 (2008) 027404.
- [23] Y. Okimoto, T. Miyata, M.S. Endo, M. Kurashima, K. Onda, T. Ishikawa, S. Koshihara, M. Lorenc, E. Collet, H. Cailleau, T. Arima, *Phys. Rev. B*, 84 (2011) 121102.
- [24] H. Uemura, H. Okamoto, *Phys. Rev. Lett.* 105 (2010) 258302.
- [25] Y. Kawakami, S. Iwai, T. Fukatsu, M. Miura, N. Yoneyama, T. Sasaki, N. Kobayashi, *Phys. Rev. Lett.* 103 (2009) 066403.
- [26] S. Decurtins, P. Güthlich, C. P. Köhler, H. Spiering, A. Hauser, *Chem. Phys. Lett.* 105 (1984) 1.
- [27] *Spin-Crossover Materials: Properties and Applications* (Ed. M. A. Halcrow), John Wiley & Sons, 2013.
- [28] I. Krivokapic, P. Chakraborty, R. Bronisz, C. Enachescu, A. Hauser, *Angew. Chem. Int. Ed.* 49 (2010) 8509-8512.
- [29] S. Cobo, D. Ostrovskii, S. Bonhommeau, L. Vendier, G. Molnar, L. Salmon, K. Tanaka, A. Bousseksou, *J. Am. Chem. Soc.* 130 (2008) 9019.
- [30] A. Cannizzo, C.J. Milne, C. Consani, W. Gawelda, Ch. Bressler, F. van Mourik, M. Chergui, *Coord. Chem. Rev.* 254 (2010) 2677.
- [31] J.J. McGarvey, I. Lawthers, K. Heremans, H. Toftlund, *J. Chem. Soc., Chem. Commun.* (1984) 1575.
- [32] M. Khalil, M.M. Marcus, A.L. Smeigh, J.K. McCusker, H.H.W. Chong, R.W. Schoenlein, *J. Phys. Chem. A*. 110 (2006) 38.
- [33] A.L. Smeigh, M. Creelman, R.A. Mathies, J.K. McCusker, *J. Am. Chem. Soc.* 130 (2008) 14105.

Edited May 24

- [34] W. Gawelda, A. Cannizzo, V.T. Pham, F. van Mourik, C. Bressler, M. Chergui, *J. Am. Chem. Soc.* 129 (2007) 8199.
- [35] M.M.N. Wolf, R. Groß, C. Schumann, J.A. Wolny, V. Schünemann, A. Døssing, H. Paulsen, J.J. McGarvey, R. Diller, *Phys. Chem. Chem. Phys.* 10 (2008) 4264.
- [36] M. Chergui, in: M. A. Halcrow (Eds.), *Spin-crossover Materials*, Wiley, West Sussex, 2013, 405-489.
- [37] C. Brady, H. Toftlund, J.J. McGarvey, J.K. McCusker, D.N. Hendrickson, in: P. Gütlich, H.A. Goodwin (Eds.), *Spin-crossover in Transition Metal Compounds*, vol. III, Springer, Berlin, 2004, p. 1, *Top. Curr. Chem.*, 235.
- [38] C. Consani, M. Prémont-Schwarz, A. Elnahhas, C. Bressler, F. van Mourik, A. Cannizzo, M. Chergui, *Angew. Chem. Int. Ed.* 48 (2009) 7184.
- [39] J.K. McCusker, K.N. Walde, R.C. Dunn, J.D. Simon, D. Madge, D.N. Hendrickson, *J. Am. Chem. Soc.* 114 (1992) 6919.
- [40] J.E. Monat, J.K. McCusker, *J. Am. Chem. Soc.* 122 (2000) 4092.
- [41] I. Lawthers, J. J. McGarvey, *J. Am. Chem. Soc.* 15 (1984) 106.
- [42] N. Huse, H. Cho, K. Hong, L. Jamula, F.M.F. de Groot, T.K. Kim, J.K. McCusker, R.W. Schoenlein, *J. Phys. Chem. Lett.* 2 (2011) 880.
- [43] W. Gawelda, V. T. Pham, M. Benfatto, Y. Zaushitsyn, M. Kaiser, D. Grolimund, S. L. Johnson, R. Abela, A. Hauser, C. Bressler, M. Chergui, *Phys. Rev. Lett.* 98 (2007) 057401.
- [44] S. Nozawa, T. Sato, M. Chollet, K. Ichiyanagi, A. Tomita, H. Fujii, S. I. Adachi, S.Y. Koshihara, *J. Am. Chem. Soc.* 132 (2010) 61.
- [45] H.T. Lemke, C. Bressler, L.X. Chen, D.M. Fritz, K.J. Gaffney, A. Galler, W. Gawelda, K. Haldrup, R.W. Hartsock, H. Ihee, J. Kim, K.H. Kim, J.H. Lee, M.M. Nielsen, A.B. Stickrath, W. Zhang, D. Zhu, M. Cammarata, *J. Phys. Chem. A* 117 (2013) 735.
- [46] C. Bressler, C. Milne, V. T. Pham, A. El Nahhas, R.M. van der Veen, W. Gawelda, S. Johnson, P. Beaud, D. Grolimund, M. Kaiser, C. Borca, G. Ingold, R. Abela, M. Chergui, *Science* 323 (2009) 489.
- [47] E. A. Juban, A. L. Smeigh, J. E. Monat, J. K. McCusker, *Coord. Chem. Rev.* 250 (2006) 1783.
- [48] N. Huse, T.K. Kim, L. Jamula, J.K. McCusker, F.M. F. de Groot, R.W. Schoenlein, *J. Am. Chem. Soc.* 132 (2010) 6809.
- [49] N. Bréfuel, H. Watanabe, L. Toupet, J. Come, M. Kojima, N. Matsumoto, E. Collet, K. Tanaka, J.P. Tuchagues, *Ang. Chem. Int. Ed.* 48 (2009) 9304.
- [50] E. Collet, H. Watanabe, N. Bréfuel, L. Palatinus, F. Roudaut, L. Toupet, K. Tanaka, J.P. Tuchagues, P. Fertey, S. Ravy, B. Toudic, H. Cailleau, *Phys. Rev. Lett.* 109 (2012) 257206.
- [51] M. Buron-Le Cointe, J. Hébert, C. Baldé, N. Moisan, L. Toupet, P. Guionneau, J.F. Létard, E. Freysz, H. Cailleau, E. Collet, *Phys. Rev. B* 85 (2012) 064114.
- [52] O. Fouché, J. Degert, G. Jonusauskas, N. Daro, J. F. Létard, E. Freysz, *Phys. Chem. Chem. Phys.* 12 (2010) 3044.
- [53] R. Bertoni, A. Lorenc, A. Tissot, M. Servol, M.-L. Boillot, E. Collet, *Angew. Chem. Int. Ed.* 51 (2012) 7485.
- [54] A. Marino, P. Chakraborty, M. Servol, M. Lorenc, E. Collet, A. Hauser, *Angew. Chem. Int. Ed.* 2014 doi: 10.1002/anie.201310884
- [55] M. Lorenc, C. Balde, W. Kaszub, A. Tissot, Moisan, M. Servol, M. Buron-Le Cointe, H. Cailleau, P. Chasle, P. Czarnecki, M. L. Boillot, E. Collet, *Phys. Rev. B* 85 (2012) 054302.
- [56] H. Cailleau, M. Lorenc, L. Guérin, M. Servol, E. Collet, M. Buron-Le Cointe, *Acta Cryst. A* 66 (2010) 189.
- [57] E. Collet, M. Lorenc, M. Cammarata, L. Guérin, M. Servol, A. Tissot, M.L. Boillot, H. Cailleau, M. Buron, *Chemistry: A European Journal* 18 (2012) 2051.
- [58] E. Collet, N. Moisan, C. Baldé, R. Bertoni, E. Trzop, C. Laulhé, M. Lorenc, M. Servol, H. Cailleau, A. Tissot, M.L. Boillot, T. Graber, R. Henning, P. Coppens, M. Buron, *Phys. Chem. Chem. Phys.* 14 (2012) 6192.

Edited May 24

- [59] A. Marino, M. Servol, R. Bertoni, M. Lorenc, C. Mauriac, J.F. L  tard, E. Collet, *Polyhedron* 66 (2013) 123.
- [60] W. Kaszub, M. Buron-Le Cointe, M. Lorenc, M. L. Boillot, M. Servol, A. Tissot, L. Gu  rin, H. Cailleau, E. Collet, *Eur. J Inorg. Chem* 5 (2013) 992.
- [61] E. Collet, M.L. Boillot, J. Hebert, N. Moisan, M. Servol, M. Lorenc, L. Toupet, M. Buron-Le Cointe, A. Tissot, J. Sainton, *Acta Cryst. B* 65 (2009) 474.
- [62] A. Tissot, R. Bertoni, E. Collet, L. Toupet, M.L. Boillot, *J. Mat. Chem.* 35 (2011) 2333.
- [63] M.S. Haddad, M.W. Lunch, W.D. Federer, D.N. Hendrickson, *Inorg.Chem.* 20 (1981)123.
- [64] H. Ando, Y. Nakao, H. Sato, S. Sakaki, *J. Phys. Chem. A* 111 (2007) 5515.
- [65] A. J. Simaan, M.-L. Boillot, R. Carrasco, J. Cano, J.-J. Girerd, T. A. Mattioli, J. Ensling, H. Spiering, P. G  tlich, *Chem. Eur. J.* 11 (2005) 1779.
- [66] A. Tissot, C. Enachescu, M-L. Boillot, 22 (2012) 20451-20457.
- [67] A. Hauser in: P. G  tlich, H.A. Goodwin (Eds.), *Spin-crossover in Transition Metal Compounds*, vol. II, Springer, Berlin, 2004, p. 155, *Top. Curr. Chem.*, 234.
- [68] H. Okamoto, Y. Ishige, S. Tanaka, H. Kishida, S. Iwai, Y. Tokura, *Phys. Rev. B* 70 (2004) 165202.
- [69] M. Chollet, L. Guerin, N. Uchida, S. Fuhaya, H. Shimoda, T. Ishikawa, K. Matsuda, T. Hasegawa, A. Ota, H. Yamochi, G. Saito, R. Tazaki, S. Adachi, S. Koshihara, *Science* 307 (2005) 86.
- [70] B.Freyer, F.Zamponi, V. Juv  , J.Stingl, M.Woerner, T.Elsaesser, M.Chergui, *J. Chem. Phys.* 138 (2013) 144504.
- [71] C. Bressler, C. Milne, V.-T. Pham, A. El Nahhas, R. M. van der Veen, W. Gawelda, S. Johnson, P. Beaud, D. Grolimund, M. Kaiser, C. N. Borca, G. Ingold, R. Abela and M. Chergui, *Science* 323 (2009) 489.
- [72] N.Huse, H. Cho, K. Hong, L.Jamula, F. M. F. de Groot, T. K. Kim, J. K. McCusker, R. W. Schoenlein, *J. Phys. Chem. Lett.* 2(2011),880–884.
- [73] H. T. Lemke, C. Bressler, L. X. Chen, D. M. Fritz, K. J. Gaffney, A. Galler, W. Gawelda, K. Haldrup, R. W.Hartsock, H. Ihee, J. Kim, K.-H. Kim, J.-H. Lee, M. M. Nielsen, A. B. Stickrath, W. Zhang, D. Zhu, M. Cammarata, *J. Phys. Chem. A* 117 (2013) 735-740.
- [74] J.J. McGarvey, I. Lawthers, K. Heremans, H. Toflund, *Inorg. Chem.* 29 (1990) 252.
- [75] H. Toflund, *Coord. Chem. Rev.* 97 (1989) 67.
- [76] E.V. Dose, M.A. Hoselton, N. Sutin, M.F. Tweedle, L.J. Wilson, *J. Am. Chem. Soc.* 100 (1978) 1141.
- [77] J.K. Beattie, K.J. McMahon, *Austr. J. Chem.* 41 (1989) 1315; J.K. Beattie *Adv. Inorg. Chem.* 1988, 32, 1-53.
- [78] J. J. McGarvey, I. J. Lawthers, *Chem. Soc., Chem. Commun.* (1982) 906.

- An overview spin-state photo-switching in Fe^{III} spin-crossover crystals is provided
- Ultrafast optical spectroscopy reveal a sequence of conversion
- Lattice expansion and heating induce additional spin-state conversion
- The photo-response is linear with excitation density
- The thermal conversion is strong in cooperative materials close to phase transition

Accepted Manuscript